CERN-TH-2025-152, TTP25-024, P3H-25-052

The SN 1987A Cooling Bound on Dark Matter Absorption in Electron Targets

Claudio Andrea Manzari,[1,2,*] Jorge Martin Camalich,[3,4,5,†] Jonas Spinner,[6,‡] and Robert Ziegler[6,7,§]

[1] *Berkeley Center for Theoretical Physics, Department of Physics, University of California, Berkeley, CA 94720, USA*
[2] *Theoretical Physics Group, Lawrence Berkeley National Laboratory, Berkeley, CA 94720, USA*
[3] *Instituto de Astrofísica de Canarias, C/ Vía Láctea, s/n E38205 - La Laguna, Tenerife, Spain*
[4] *Universidad de La Laguna, Departamento de Astrofísica, La Laguna, Tenerife, Spain*
[5] *CERN, Theoretical Physics Department, CH-1211 Geneva 23, Switzerland*
[6] *Institut für Theoretische Physik, Universität Heidelberg, Germany*
[7] *Institut für Theoretische Teilchenphysik, Karlsruhe Institute of Technology, Karlsruhe, Germany*

We present new supernova (SN 1987A) cooling bounds on sub-MeV fermionic dark matter with effective couplings to electrons. These bounds probe the parameter space relevant for direct detection experiments in which dark matter can be absorbed by the target material, showing strong complementarity with indirect searches and constraints from dark matter overproduction. Crucially, our limits exclude the projected sensitivity regions of current and upcoming direct detection experiments. Since these conclusions are *a priori* not valid for light mediators, we extend our analysis to this case. We show that sub-GeV mediators can be produced resonantly both in supernova cores and in the early Universe, altering the SN 1987A analysis for effective couplings. Still, a combination of supernova cooling constraints and limits from dark matter overproduction excludes the entire parameter space relevant for direct detection in this case.

The nature of dark matter (DM) remains elusive to this day. Direct detection (DD) experiments have pushed the limits on elastic scattering cross sections on nucleons close to the neutrino floor for multi-GeV DM. Combined with the so-far negative searches for particles with weak-scale masses at colliders and in astrophysical indirect detection (ID), the present experimental situation motivates the exploration of alternative DM scenarios beyond the classic WIMP paradigm (see, e.g. Refs. [1, 2]).

One of the prominent emerging directions involves candidates with masses below 1 GeV. For such light DM, nuclear recoil signals in DD experiments typically fall below detection thresholds, which are often of the order of $\mathcal{O}$(keV) and, as a result, sub-GeV DM remains largely unconstrained by conventional experimental techniques. This challenge has motivated the development of lower-threshold detectors and alternative scattering targets [3–42], leading to a surge of theoretical activity in sub-GeV DM model building (see, e.g. Refs. [43–45]).

An interesting class of sub-GeV DM scenarios accessible by current experimental techniques is based on the absorption of DM in the target material [46–48]. The rest mass of the DM particle is then converted into recoil energy, which becomes as large as $T_r \sim m_\chi^2/2m_T$, where m_T is the mass of the target and $m_\chi \ll m_T$ the mass of the DM particle. Absorption in nuclear targets thus probes DM masses down to $\mathcal{O}$(MeV) [47, 49], while absorption on electrons in conventional liquid xenon DD experiments such as XENON1T [50], LZ [51], XENONnT [52], PandaX-4T [53] and DARWIN [54] gives sensitivity to DM masses in the sub-MeV range.

The possibility of DM absorption on electrons necessarily implies that DM is unstable. While decays to electrons can be avoided for DM with masses below threshold, $m_\chi \leq 2m_e$, loop-induced decays to photons and neutrinos are unavoidable. These scenarios are constrained by ID through X-ray and γ-ray telescopes, as well as by their imprints on the cosmological history. Interestingly, DM in this mass range can also be produced in extreme astrophysical environments, such as the hot and dense proto-neutron stars (PNS) formed during core-collapse supernovae (SN). Although limits on DM couplings have been extensively studied in the literature for light bosonic DM (see e.g. Ref. [55–66]), similar arguments for dark fermions have been much less explored (for early works see Refs. [67–69]). In fact, SNe can play a significant role in probing these DM models, opening new search strategies that are complementary to DD, ID, and collider searches [70–74].

In this Letter, we present a novel application of the classic SN cooling limit [75] for sub-MeV fermionic DM coupled to electrons. We focus on the models proposed in Ref. [46], where absorption of DM particles leads to striking signatures in DD experiments. Following the relevant studies in Ref. [46, 48, 76] we parametrize the DM-electron interactions in a model-independent way by the following effective field theory (EFT) Lagrangian

$$\mathcal{L}_\chi = \sum_X \frac{1}{\Lambda_X^2} \left(\bar{e}\,\Gamma_X e\right) \cdot \left(\bar{\chi}\,\Gamma_X \nu_L\right) + \text{h.c.}\,, \tag{1}$$

where e and ν_L are the Standard Model (SM) electron and neutrino fields, χ is the DM fermion, and the interactions are parametrized by the effective UV scale Λ_X and the Dirac matrix Γ_X.

We focus our analysis on the vector operator, $\Gamma_X = \Gamma_V = \gamma_\mu$, and scalar operator $\Gamma_X = \Gamma_S = \mathbb{1}$, both of which have been probed in DD by PandaX [77, 78] and CDEX [79], as well as in ID [76]. Our derivation of SN cooling limits can be extended to other operators, includ-

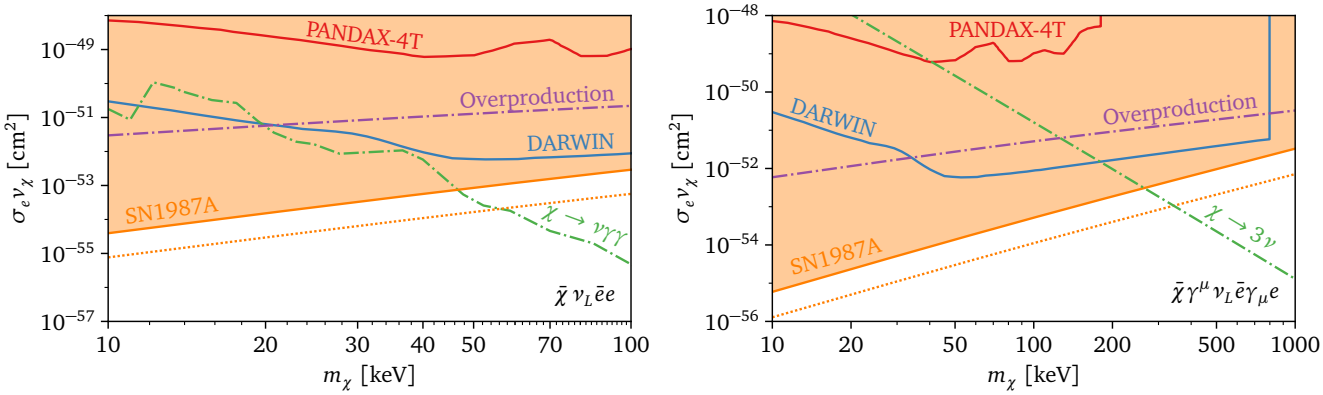

FIG. 1. SN 1987A cooling constraints for scalar (left) and vector (right) interactions compared to DD searches by PANDA4T-X and prospects from DARWIN. The dotted line covers the estimated uncertainty from using different SN models. Other upper bounds include cosmological overproduction (see text and SupM for details) and those from ID derived in Ref. [76].

ing those in which we replace the SM neutrino by a sterile one ν_R [48]. In the supplemental material (SupM), we present the analysis of these operators for completeness.

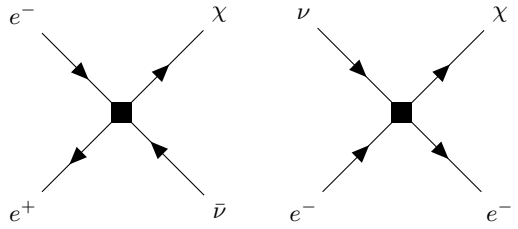

FIG. 2. Feynman diagrams for production of DM particles χ in the PNS for the interactions in Eq. (1), referred to as *annihilation* (left) and *scattering* (right) processes, respectively.

DM interacting with the SM through Eq. (1) can be produced in SNe. A bound on Λ_X then follows from the classic SN cooling upper limit: the luminosity induced by the emission of DM particles should be lower than the neutrino luminosity, $L_\chi \lesssim L_\nu$, at 1 sec post-bounce, to be consistent with the neutrino emission signal detected during SN 1987A [75]. Here, both L_ν and L_χ depend on the numerical values of the thermodynamical parameters used in the underlying SN simulation.

The SN 1987A bounds on Λ_X can be converted to limits on the scattering cross section probed in DD, as shown in Fig. 1. These bounds clearly lie within the region probed by DD experiments and are strongly complementary to other astrophysical ID and cosmological limits. In particular, they exclude the whole range of cross sections accessible to current and future DD searches across the full mass window $10\,\text{keV} \lesssim m_\chi \lesssim 1\,\text{GeV}$.

For the numerical analysis shown in this figure, we use SN simulations from Ref. [80]. Specifically, we employ the radial profiles of thermodynamic quantities provided for the coolest and hottest PNS, corresponding to the SFHo18.80 and SFHo20.0 models, respectively. These profiles are used to compute the dark luminosity $L_\chi = \int dV (Q_\chi + Q_{\overline{\chi}})$ as a function of the coupling scale Λ_X, assuming neutrino luminosities of $L_\nu = 5.7 \times 10^{52}$ erg/s for SFHo18.80 and $L_\nu = 1.0 \times 10^{53}$ erg/s for SFHo20.0. In the following, we describe these calculations and the derivation of our limits in Fig. 1 in detail.

Dark luminosity in the free-streaming regime – The Feynman diagrams that contribute to the thermal production of χ's in the core of PNS are shown in Fig. 2. If the χ particles interact weakly, they freely stream out of the inner core, leading to an energy loss rate per unit volume Q. Therefore, DM is produced by processes $\psi_1\psi_2 \to \psi_3\chi$, where ψ_i are SM fermions and

$$Q = \int \Big[\prod_{i=1}^{4} \frac{d^3\vec{p}_i}{(2\pi)^3 2E_i}\Big](2\pi)^4\delta^4(p_1+p_2-p_3-p_\chi) \times f_1 f_2 (1-f_3) \sum_{\text{spins}} |\mathcal{M}|^2 E_\chi \,. \quad (2)$$

The $p_i = (E_i, \vec{p}_i)$ are the 4-momentum of the particles labeled by i, with $i = 4$ corresponding to the χ. The squared matrix elements $|\mathcal{M}|^2$, summed over all fermion spins, encode the interactions that produce the scattering process, while the Fermi-Dirac occupation numbers $f_i^{-1} = \exp(E_i - \mu_i)/T + 1$ describe the local themodynamic equilibrium conditions of the PNS parametrized by the chemical potential μ_i and temperature T.

The energies E_i are defined in the rest frame of the PNS, where the initial particles collide with 3-momenta $\vec{p}_1$ and $\vec{p}_2$ forming an angle θ. The energy loss rate can then be factorized as (cf. Ref. [71])

$$Q = \frac{1}{32\pi^4} \int_{m_1}^{\infty} dE_1 \bar{p}_1 f_1 \int_{m_2}^{\infty} dE_2 \bar{p}_2 f_2 \int_{-1}^{1} dc_\theta \Theta_s J_s \,, \quad (3)$$

where $\bar{p}_i = |\vec{p}_i|$, m_i are the masses and $c_\theta = \cos\theta$. The function J_s contains the dynamical information on the scattering process

$$J_s(E_1, E_2, s) = \frac{\bar{p}'_{34}}{16\pi^2\sqrt{s}} \int_{-1}^{1} dc_{\theta'} \int_0^{2\pi} d\phi' (1 - f_3) \times \sum_{\text{spins}} |\mathcal{M}(s,t)|^2 E_\chi \,. \quad (4)$$

where $s = (p_1 + p_2)^2$ and $t = (p_1 - p_3)^2$ are the Mandelstam variables and the Heavyside function $\Theta_s \equiv \theta(s - (m_1 + m_2)^2)\theta(s - (m_3 + m_\chi)^2)$ enforces kinematic thresholds. In this equation, primed variables refer to the center-of-mass frame and $\bar{p}'_{34}$ is the corresponding absolute value of the final state 3-momentum. The variables in the PNS frame E_3 (hidden in f_3) and E_χ can be expressed as functions of E_1, E_2, s before integrating over the angles θ' and ϕ', see SupM for more details.

Significant simplifications of Eq. (4) can be obtained by employing two approximations:

i) **Degeneracy factorization:** replacing the Pauli-blocking factor $(1 - f_i)$ by its thermal average [75]

$$(1 - f_i) \to F_i \equiv \frac{\mathfrak{g}_i}{n_i} \int \frac{d^3\vec{p}_i}{(2\pi)^3} f_i (1 - f_i) \,. \quad (5)$$

where $\mathfrak{g}_i$ is the number of degrees of freedom and n_i the number density. For *typical* PNS conditions ($T = 30$ MeV, $\mu_e = 130$ MeV, $\mu_{\nu_e} = 20$ MeV) $F_{e^-} = 0.53, F_{\nu_e} = 0.86$, which is a moderate effect.

ii) **Massless limit:** all particles can be taken as massless, since for the DM mass range of interest $m_\nu, m_e, m_\chi \ll T,\ \mu_i$ in SN.

These approximations lead to simple analytical formulae for the contributions to Q from the two processes in Fig. (2). For the *annihilation* process $e^+e^- \to \nu\bar{\chi}$ ($e^+e^- \to \bar{\nu}\chi$) one finds

$$Q_{\text{an}} = \frac{a_X\, T^9 F_{\nu(\bar{\nu})}}{18\pi^5 \Lambda_X^4} H_4(y_e) H_3(-y_e) + (y_e \to -y_e) \,, \quad (6)$$

where $y_i = \mu_i/T$, $a_V = 1$ or $a_S = 3/4$, and

$$H_n(y) = \int_0^\infty dx \frac{x^n}{1 + e^{x-y}} = -n!\, \text{Li}_{n+1}(-e^y) \,. \quad (7)$$

For the *scattering* process $e^-\nu \to e^-\chi$ one obtains

$$Q_{\text{sc}} = \frac{T^9 F_{e^-}}{72\pi^5 \Lambda_X^4} \left[b_X H_4(y_e) H_3(y_\nu) + c_X H_4(y_\nu) H_3(y_e) \right] , \quad (8)$$

where $b_V = 7$, $c_V = 9$, and $b_S = 3/2$, $c_S = 1/2$. Other channels like $e^-\bar{\nu} \to e^-\bar{\chi}$ or $e^+\nu \to e^+\chi$ are obtained from Eq. (8) by replacing the arguments of the $H_n(y)$ functions accordingly. Compared to annihilation in Eq. (6), the contribution of electron scattering to the energy-loss rate does not suffer the strong suppression due to the small positron abundance, and is only slightly suppressed by partial electron degeneracy. Indeed, for *typical* PNS conditions $H_4(y_e) \approx 1040$, $H_3(y_e) \approx 192$ but $H_4(-y_e) \approx 0.3$, $H_3(-y_e) \approx 0.08$, compared to the neutrino conditions $H_4(y_{\nu_e}) \approx 44$ and $H_3(y_{\nu_e}) \approx 11$. Therefore, neutrino scattering on electrons provides the leading contribution to Q, while scattering on anti-neutrinos gives a rate smaller by about a factor 4, for nominal conditions in the PNS.

Adding the contributions in Q_{an} and Q_{sc} one obtains

$$\Lambda_S \gtrsim (9.3 - 14)\ \text{TeV} \,, \quad \Lambda_V \gtrsim (15 - 22)\ \text{TeV} \,, \quad (9)$$

where the lower (upper) value correspond to the colder (hotter) simulation SFHo18.80 (SFHo20.0) [80].

Dark luminosity in the trapping regime – In the trapping regime the DM particles reach thermal equilibrium with the plasma in the PNS and are emitted from a surface with radius r_χ (the *dark sphere*) following a law analogous to black-body radiation. Including the degrees of freedom of approximately massless χ and $\bar{\chi}$, this reads

$$L_\chi^{\text{trap}} = \frac{7\pi^3}{30} r_\chi^2 T_\chi^4 \,, \quad (10)$$

where $T_\chi = T(r_\chi)$ and the radius r_χ is defined by requiring the optical depth to be $\tau_\chi(r_\chi) = \int_{r_\chi}^\infty dr/\lambda(r) = 2/3$ [81–83], where $\lambda(r)$ is a suitable spectral average of the DM's mean free path (MFP) at a radius r. Here we use a "naive" thermal average

$$\lambda(r) = \frac{\mathfrak{g}_\chi}{n_\chi} \int \frac{d^3\vec{p}_\chi}{(2\pi)^3} f_\chi \lambda(r, E_\chi) \,. \quad (11)$$

The energy-dependent MFP $\lambda(r, E_\chi)$ is related to the total absorption rate of DM particles in the medium, $\Gamma = 1/\lambda$. Given the thermodynamical conditions of the plasma at radius r, the rate for $\chi\psi_1 \to \psi_2\psi_3$ is

$$\Gamma(E_\chi) = \frac{1}{2E_\chi \mathfrak{g}_\chi} \int \left[\prod_{i=1}^3 \frac{d^3\vec{p}_i}{(2\pi)^3 2E_i} \right] f_1 (1 - f_2)(1 - f_3) \times (2\pi)^4 \delta^4(p_1 + p_2 - p_3 - p_\chi) \sum_{\text{spins}} |\mathcal{M}|^2 \,, \quad (12)$$

where the particle $i = 1$ is identified with the SM scatterer and $i = 2, 3$ with the final SM particles, and where $\mathcal{M}$ is the scattering amplitude of the process. Following an analysis similar to Eq. (3) we find

$$\Gamma(E_\chi) = \frac{1}{16\pi^2 E_\chi \mathfrak{g}_\chi} \int_{m_1}^\infty dE_1 \bar{p}_1 f_1 \int_{-1}^1 dc_\theta \Theta_s K_s \,, \quad (13)$$

where $\Theta_s \equiv \theta(s-(m_2+m_3)^2)\theta(s-(m_1+m_\chi)^2)$ and

$$K_s(E_\chi, E_1, s) = \frac{\bar{p}'_{23}}{16\pi^2\sqrt{s}} \int_{-1}^{1} dc_{\theta'} \int_0^{2\pi} d\phi' (1-f_2)(1-f_3) \times \sum_{\text{spins}} |\mathcal{M}(s,t)|^2 \,. \tag{14}$$

Using the same approximations as for Q one obtains

$$\Gamma_{\text{an}}(E_\chi) = \frac{2a_X E_\chi T^4 F_e F_{\bar{e}}}{9\pi^3 \Lambda_X^4 \mathfrak{g}_\chi} H_3(-y_\nu),$$
$$\Gamma_{\text{sc}}(E_\chi) = \frac{4d_X E_\chi T^4 F_\nu F_e}{9\pi^3 \Lambda_X^4 \mathfrak{g}_\chi} H_3(y_e), \tag{15}$$

for *inverse annihilation*, $\chi\bar{\nu} \to e^+e^-$, and *inverse scattering*, $\chi e^- \to \nu e^-$ (with coeffcients $d_V = 1$ and $d_S = 1/8$), respectively and where we have assumed that DM is in chemical equilibrium, $\mu_\chi = \mu_\nu$. One finds that the SN 1987A constraint has a lower bound at

$$\Lambda_S \lesssim (38-41)\ \text{GeV}\,,$$
$$\Lambda_V \lesssim (56-59)\ \text{GeV}\,, \tag{16}$$

for the simulations SFHo18.80 and SFHo20.0 [80].

Results and discussion – The SN 1987A cooling limits derived above can be converted to upper limits on the DD cross section predicted in the EFT [76]. The results for vector and scalar operators shown in Fig. 1 demonstrate that the new SN bound covers a large fraction of the previously unconstrained region of interest for ID, and current and future DD experiments (i.e. DARWIN [54]).

The cosmological overabundance limits in Fig. 1 are obtained assuming that DM is produced in the early Universe via UV freeze-in by the *same* mechanisms as in SN, *cf.* Fig. 2. Our limits, derived in the SupM, are more stringent than those reported in previous studies [48, 76].

One important caveat in our analysis, concerning the validity of the results shown in Fig. 1, is the use of EFT. While this approximation holds in DD and ID, where the relevant energy scale (set by the DM mass) is assumed to be much smaller than the mediator mass, it can break down in the context of thermal production of DM in the PNS, where temperatures can reach $\mathcal{O}(10\,\text{MeV})$.

In Fig. 3 we show the limits on a simplified UV completion of the scalar operator, with interactions mediated by a real scalar Φ,

$$\mathcal{L}_S \supset y_e \bar{e} e \Phi + y_\chi \bar{\chi} \nu_L \Phi + \text{h.c.}\,, \tag{17}$$

for a given DM mass $m_\chi = 20$ keV and as a function of the mediator mass m_Φ. For heavy mediators above ≈ 1 GeV (≈ 100 MeV) the SN cooling limits become independent of the mediator mass and approach the results of the EFT calculation for the free-streaming (trapping regime). However, for light mediators the bound departs strongly from the EFT behavior. The physical reason for

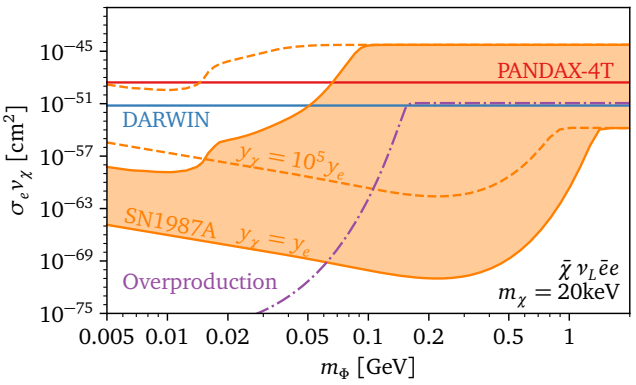

FIG. 3. Bounds on the DD cross-section for the absorption of DM with $m_\chi = 20$ keV and sub-GeV scalar mediator. For $y_e = y_\chi$, the SN 1987A limits from SFHo18.80 are compared to the limit from DM overproduction and sensitivity limits achieved by PANDAX-4T and the prospects for DARWIN. We also show the SN 1987A bound obtained using $y_\chi = 10^5 y_e$ or vice-versa. For such hierarchical couplings the overproduction bound would only get stronger.

this change is the onset of resonant production processes in annihilation $e^+e^- \to \Phi^* \to \chi\bar{\nu}$ and photo-production $e^-\gamma \to e^-\Phi^*(\to \chi\bar{\nu})$ [71], described for completeness in the SupM. The production and absorption rates in SN in this resonant regime scale quadratically (and not quartically) with the couplings and the bound covers a region of couplings much smaller than what could have been naively expected from the EFT. Therefore, as shown in Fig. 3, SN 1987A does not constrain the region accessible to DD for light mediators with $m_\Phi \lesssim 70$ MeV, unless there are large hierarchies in the couplings.

However, as stressed above, the same processes underlying DM production in the PNS will produce DM in the early Universe through freeze-in. The temperatures dominating the cosmological DM production are around the reheating temperature, $T_R \gtrsim 5$ MeV, which are similar to those in SN, and cosmological DM production is also resonantly enhanced for light mediators [84]. This is shown in Fig. 3 where the overproduction bound is drastically strengthened due to this resonant behavior for $m_\Phi \lesssim 150$ MeV, excluding the region of interest for DD.

In conclusion, in this work, we have presented new SN 1987A cooling bounds on sub-MeV fermionic dark matter with effective couplings to electrons. Importantly, our bounds exclude a significant fraction of the projected sensitivity regions of both current and future DD experiments and are highly complementary to ID searches with X-ray and γ-ray telescopes and cosmological limits. We have corroborated these conclusions obtained in the EFT by exploring how these constraints are affected in simple UV completions with sub-GeV mediators. While these mediators can be produced on-shell in supernova cores, shifting the constrained regions to smaller couplings, the same resonant behavior occurs in the early

Universe, strengthening the overproduction limits. As a result, the parameter space accessible to direct detection remains excluded.

Our results highlight the important role that SN analyses can play in probing sub-GeV DM scenarios beyond the reach of traditional laboratory and cosmological searches.

ACKNOWLEDGMENTS

We thank Filippo Sala for useful discussions and Robert Bollig and Hans Thomas Janka for sharing data of the simulations with us. JMC also acknowledges CERN-TH for hospitality during the completion of this article. This work is partially supported by project B3a of the DFG-funded Collaborative Research Center TRR257, "Particle Physics Phenomenology after the Higgs Discovery" and has received support from the European Union's Horizon 2020 research and innovation programme under the Marie Skłodowska -Curie grant agreement No 860881-HIDDeN. The work of C.A.M. is supported by the Office of High Energy Physics of the U.S. Department of Energy under contract DE- AC02-05CH11231. JMC acknowledge support from the MICINN through the grant "DarkMaps" PID2022-142142NB-I00 and from the European Union through the grant "UNDARK" of the Widening participation and spreading excellence programme (project number 101159929). J.S. is funded by the Carl-Zeiss-Stiftung through the project *Model-Based AI: Physical Models and Deep Learning for Imaging and Cancer Treatment*.

Note added – While this work was being finalized, an independent analysis of SN 1987A bounds on the same effective models appeared as a preprint [85]. Compared to their results, our bounds are approximately one to two orders of magnitude weaker (depending on the SN simulation used). Our supernova analysis is more systematic, extends to the case of simple UV completions and sterile neutrinos, and we derive consistently the relevant cosmological limits from overproduction. In particular, we discuss the implications of light mediators where the EFT analysis breaks down.

* camanzari@berkeley.edu
† jcamalich@iac.es
‡ j.spinner@thphys.uni-heidelberg.de
§ robert.ziegler@kit.edu

[1] Marco Cirelli, Alessandro Strumia, and Jure Zupan, "Dark Matter," (2024), arXiv:2406.01705 [hep-ph].
[2] Giorgio Arcadi, David Cabo-Almeida, Maíra Dutra, Pradipta Ghosh, Manfred Lindner, Yann Mambrini, Jacinto P. Neto, Mathias Pierre, Stefano Profumo, and Farinaldo S. Queiroz, "The Waning of the WIMP: Endgame?" Eur. Phys. J. C **85**, 152 (2025), arXiv:2403.15860 [hep-ph].
[3] Rouven Essig, Jeremy Mardon, and Tomer Volansky, "Direct Detection of Sub-GeV Dark Matter," Phys. Rev. D **85**, 076007 (2012), arXiv:1108.5383 [hep-ph].
[4] Peter W. Graham, David E. Kaplan, Surjeet Rajendran, and Matthew T. Walters, "Semiconductor Probes of Light Dark Matter," Phys. Dark Univ. **1**, 32–49 (2012), arXiv:1203.2531 [hep-ph].
[5] Rouven Essig, Aaron Manalaysay, Jeremy Mardon, Peter Sorensen, and Tomer Volansky, "First Direct Detection Limits on sub-GeV Dark Matter from XENON10," Phys. Rev. Lett. **109**, 021301 (2012), arXiv:1206.2644 [astro-ph.CO].
[6] Wei Guo and Daniel N. McKinsey, "Concept for a dark matter detector using liquid helium-4," Phys. Rev. D **87**, 115001 (2013), arXiv:1302.0534 [astro-ph.IM].
[7] Yonit Hochberg, Yue Zhao, and Kathryn M. Zurek, "Superconducting Detectors for Superlight Dark Matter," Phys. Rev. Lett. **116**, 011301 (2016), arXiv:1504.07237 [hep-ph].
[8] Rouven Essig, Marivi Fernandez-Serra, Jeremy Mardon, Adrian Soto, Tomer Volansky, and Tien-Tien Yu, "Direct Detection of sub-GeV Dark Matter with Semiconductor Targets," JHEP **05**, 046 (2016), arXiv:1509.01598 [hep-ph].
[9] Yonit Hochberg, Matt Pyle, Yue Zhao, and Kathryn M. Zurek, "Detecting Superlight Dark Matter with Fermi-Degenerate Materials," JHEP **08**, 057 (2016), arXiv:1512.04533 [hep-ph].
[10] Yonit Hochberg, Tongyan Lin, and Kathryn M. Zurek, "Detecting Ultralight Bosonic Dark Matter via Absorption in Superconductors," Phys. Rev. D **94**, 015019 (2016), arXiv:1604.06800 [hep-ph].
[11] Katelin Schutz and Kathryn M. Zurek, "Detectability of Light Dark Matter with Superfluid Helium," Phys. Rev. Lett. **117**, 121302 (2016), arXiv:1604.08206 [hep-ph].
[12] Yonit Hochberg, Yonatan Kahn, Mariangela Lisanti, Christopher G. Tully, and Kathryn M. Zurek, "Directional detection of dark matter with two-dimensional targets," Phys. Lett. B **772**, 239–246 (2017), arXiv:1606.08849 [hep-ph].
[13] Stephen Derenzo, Rouven Essig, Andrea Massari, Adrían Soto, and Tien-Tien Yu, "Direct Detection of sub-GeV Dark Matter with Scintillating Targets," Phys. Rev. D **96**, 016026 (2017), arXiv:1607.01009 [hep-ph].
[14] Yonit Hochberg, Tongyan Lin, and Kathryn M. Zurek, "Absorption of light dark matter in semiconductors," Phys. Rev. D **95**, 023013 (2017), arXiv:1608.01994 [hep-ph].
[15] Simon Knapen, Tongyan Lin, and Kathryn M. Zurek, "Light Dark Matter in Superfluid Helium: Detection with Multi-excitation Production," Phys. Rev. D **95**, 056019 (2017), arXiv:1611.06228 [hep-ph].
[16] Rouven Essig, Tomer Volansky, and Tien-Tien Yu, "New Constraints and Prospects for sub-GeV Dark Matter Scattering off Electrons in Xenon," Phys. Rev. D **96**, 043017 (2017), arXiv:1703.00910 [hep-ph].
[17] Ranny Budnik, Ori Chesnovsky, Oren Slone, and Tomer Volansky, "Direct Detection of Light Dark Matter and Solar Neutrinos via Color Center Production in Crystals," Phys. Lett. B **782**, 242–250 (2018), arXiv:1705.03016 [hep-ph].
[18] G. Cavoto, F. Luchetta, and A. D. Polosa, "Sub-GeV

Dark Matter Detection with Electron Recoils in Carbon Nanotubes," Phys. Lett. B **776**, 338–344 (2018), arXiv:1706.02487 [hep-ph].
[19] Yonit Hochberg, Yonatan Kahn, Mariangela Lisanti, Kathryn M. Zurek, Adolfo G. Grushin, Roni Ilan, Sinéad M. Griffin, Zhen-Fei Liu, Sophie F. Weber, and Jeffrey B. Neaton, "Detection of sub-MeV Dark Matter with Three-Dimensional Dirac Materials," Phys. Rev. D **97**, 015004 (2018), arXiv:1708.08929 [hep-ph].
[20] Simon Knapen, Tongyan Lin, Matt Pyle, and Kathryn M. Zurek, "Detection of Light Dark Matter With Optical Phonons in Polar Materials," Phys. Lett. B **785**, 386–390 (2018), arXiv:1712.06598 [hep-ph].
[21] Masha Baryakhtar, Junwu Huang, and Robert Lasenby, "Axion and hidden photon dark matter detection with multilayer optical haloscopes," Phys. Rev. D **98**, 035006 (2018), arXiv:1803.11455 [hep-ph].
[22] Matthew Szydagis, Cecilia Levy, Yujia Huang, Alvine C. Kamaha, Corwin C. Knight, Gregory R. C. Rischbieter, and Peter W. Wilson, "Demonstration of neutron radiation-induced nucleation of supercooled water," Phys. Chem. Chem. Phys. **23**, 13440–13446 (2021), arXiv:1807.09253 [physics.ins-det].
[23] Sinead Griffin, Simon Knapen, Tongyan Lin, and Kathryn M. Zurek, "Directional Detection of Light Dark Matter with Polar Materials," Phys. Rev. D **98**, 115034 (2018), arXiv:1807.10291 [hep-ph].
[24] Noah Alexander Kurinsky, To Chin Yu, Yonit Hochberg, and Blas Cabrera, "Diamond Detectors for Direct Detection of Sub-GeV Dark Matter," Phys. Rev. D **99**, 123005 (2019), arXiv:1901.07569 [hep-ex].
[25] Francesca Acanfora, Angelo Esposito, and Antonio D. Polosa, "Sub-GeV Dark Matter in Superfluid He-4: an Effective Theory Approach," Eur. Phys. J. C **79**, 549 (2019), arXiv:1902.02361 [hep-ph].
[26] Yonit Hochberg, Ilya Charaev, Sae-Woo Nam, Varun Verma, Marco Colangelo, and Karl K. Berggren, "Detecting Sub-GeV Dark Matter with Superconducting Nanowires," Phys. Rev. Lett. **123**, 151802 (2019), arXiv:1903.05101 [hep-ph].
[27] Tanner Trickle, Zhengkang Zhang, and Kathryn M. Zurek, "Detecting Light Dark Matter with Magnons," Phys. Rev. Lett. **124**, 201801 (2020), arXiv:1905.13744 [hep-ph].
[28] Andrea Caputo, Angelo Esposito, and Antonio D. Polosa, "Sub-MeV Dark Matter and the Goldstone Modes of Superfluid Helium," Phys. Rev. D **100**, 116007 (2019), arXiv:1907.10635 [hep-ph].
[29] Ahmet Coskuner, Andrea Mitridate, Andres Olivares, and Kathryn M. Zurek, "Directional Dark Matter Detection in Anisotropic Dirac Materials," Phys. Rev. D **103**, 016006 (2021), arXiv:1909.09170 [hep-ph].
[30] Tanner Trickle, Zhengkang Zhang, Kathryn M. Zurek, Katherine Inzani, and Sinéad M. Griffin, "Multi-Channel Direct Detection of Light Dark Matter: Theoretical Framework," JHEP **03**, 036 (2020), arXiv:1910.08092 [hep-ph].
[31] Brian Campbell-Deem, Peter Cox, Simon Knapen, Tongyan Lin, and Tom Melia, "Multiphonon excitations from dark matter scattering in crystals," Phys. Rev. D **101**, 036006 (2020), [Erratum: Phys.Rev.D 102, 019904 (2020)], arXiv:1911.03482 [hep-ph].
[32] Jonathan Kozaczuk and Tongyan Lin, "Plasmon production from dark matter scattering," Phys. Rev. D **101**, 123012 (2020), arXiv:2003.12077 [hep-ph].
[33] Gordon Baym, D. H. Beck, Jeffrey P. Filippini, C. J. Pethick, and Jessie Shelton, "Searching for low mass dark matter via phonon creation in superfluid ^{4}He," Phys. Rev. D **102**, 035014 (2020), [Erratum: Phys.Rev.D 104, 019901 (2021)], arXiv:2005.08824 [hep-ph].
[34] Sinéad M. Griffin, Yonit Hochberg, Katherine Inzani, Noah Kurinsky, Tongyan Lin, and To Chin, "Silicon carbide detectors for sub-GeV dark matter," Phys. Rev. D **103**, 075002 (2021), arXiv:2008.08560 [hep-ph].
[35] Tanner Trickle, Zhengkang Zhang, and Kathryn M. Zurek, "Effective field theory of dark matter direct detection with collective excitations," Phys. Rev. D **105**, 015001 (2022), arXiv:2009.13534 [hep-ph].
[36] Simon Knapen, Jonathan Kozaczuk, and Tongyan Lin, "Migdal Effect in Semiconductors," Phys. Rev. Lett. **127**, 081805 (2021), arXiv:2011.09496 [hep-ph].
[37] Andrea Caputo, Angelo Esposito, Fulvio Piccinini, Antonio D. Polosa, and Giuseppe Rossi, "Directional detection of light dark matter from three-phonon events in superfluid ^{4}He," Phys. Rev. D **103**, 055017 (2021), arXiv:2012.01432 [hep-ph].
[38] Brian Campbell-Deem, Simon Knapen, Tongyan Lin, and Ethan Villarama, "Dark matter direct detection from the single phonon to the nuclear recoil regime," Phys. Rev. D **106**, 036019 (2022), arXiv:2205.02250 [hep-ph].
[39] Zheng-Liang Liang, Chongjie Mo, Fawei Zheng, and Ping Zhang, "Phonon-mediated Migdal effect in semiconductor detectors," Phys. Rev. D **106**, 043004 (2022), [Erratum: Phys.Rev.D 106, 109901 (2022)], arXiv:2205.03395 [hep-ph].
[40] Belina von Krosigk *et al.*, "DELight: A Direct search Experiment for Light dark matter with superfluid helium," SciPost Phys. Proc. **12**, 016 (2023), arXiv:2209.10950 [hep-ex].
[41] Kim V. Berghaus, Angelo Esposito, Rouven Essig, and Mukul Sholapurkar, "The Migdal effect in semiconductors for dark matter with masses below $\sim$ 100 MeV," JHEP **01**, 023 (2023), arXiv:2210.06490 [hep-ph].
[42] Gordan Krnjaic, Duncan Rocha, and Tanner Trickle, "The non-relativistic effective field theory of dark matter-electron interactions," JHEP **03**, 165 (2025), arXiv:2407.14598 [hep-ph].
[43] Simon Knapen, Tongyan Lin, and Kathryn M. Zurek, "Light Dark Matter: Models and Constraints," Phys. Rev. D **96**, 115021 (2017), arXiv:1709.07882 [hep-ph].
[44] Tongyan Lin, "Dark matter models and direct detection," PoS **333**, 009 (2019), arXiv:1904.07915 [hep-ph].
[45] Kathryn M. Zurek, "Dark Matter Candidates of a Very Low Mass," Ann. Rev. Nucl. Part. Sci. **74**, 287–319 (2024), arXiv:2401.03025 [hep-ph].
[46] Jeff A. Dror, Gilly Elor, and Robert Mcgehee, "Directly Detecting Signals from Absorption of Fermionic Dark Matter," Phys. Rev. Lett. **124**, 18 (2020), arXiv:1905.12635 [hep-ph].
[47] Jeff A. Dror, Gilly Elor, and Robert Mcgehee, "Absorption of Fermionic Dark Matter by Nuclear Targets," JHEP **02**, 134 (2020), arXiv:1908.10861 [hep-ph].
[48] Jeff A. Dror, Gilly Elor, Robert McGehee, and Tien-Tien Yu, "Absorption of sub-MeV fermionic dark matter by electron targets," Phys. Rev. D **103**, 035001 (2021), [Erratum: Phys.Rev.D 105, 119903 (2022)], arXiv:2011.01940 [hep-ph].
[49] E. Adams *et al.* (PICO), "Absorption of Fermionic Dark

Matter in the PICO-60 C3F8 Bubble Chamber," Phys. Rev. Lett. **135**, 011001 (2025), arXiv:2504.13089 [hep-ex].
[50] E. Aprile *et al.* (XENON), "Light Dark Matter Search with Ionization Signals in XENON1T," Phys. Rev. Lett. **123**, 251801 (2019), arXiv:1907.11485 [hep-ex].
[51] D. S. Akerib *et al.* (LZ), "The LUX-ZEPLIN (LZ) Experiment," Nucl. Instrum. Meth. A **953**, 163047 (2020), arXiv:1910.09124 [physics.ins-det].
[52] E. Aprile *et al.* (XENON), "Projected WIMP sensitivity of the XENONnT dark matter experiment," JCAP **11**, 031 (2020), arXiv:2007.08796 [physics.ins-det].
[53] Hongguang Zhang *et al.* (PandaX), "Dark matter direct search sensitivity of the PandaX-4T experiment," Sci. China Phys. Mech. Astron. **62**, 31011 (2019), arXiv:1806.02229 [physics.ins-det].
[54] J. Aalbers *et al.* (DARWIN), "DARWIN: towards the ultimate dark matter detector," JCAP **11**, 017 (2016), arXiv:1606.07001 [astro-ph.IM].
[55] Jae Hyeok Chang, Rouven Essig, and Samuel D. McDermott, "Revisiting Supernova 1987A Constraints on Dark Photons," JHEP **01**, 107 (2017), arXiv:1611.03864 [hep-ph].
[56] Jae Hyeok Chang, Rouven Essig, and Samuel D. McDermott, "Supernova 1987A Constraints on Sub-GeV Dark Sectors, Millicharged Particles, the QCD Axion, and an Axion-like Particle," JHEP **09**, 051 (2018), arXiv:1803.00993 [hep-ph].
[57] Djuna Croon, Gilly Elor, Rebecca K. Leane, and Samuel D. McDermott, "Supernova Muons: New Constraints on Z' Bosons, Axions and ALPs," JHEP **01**, 107 (2021), arXiv:2006.13942 [hep-ph].
[58] Jorge Martin Camalich, Jorge Terol-Calvo, Laura Tolos, and Robert Ziegler, "Supernova Constraints on Dark Flavored Sectors," Phys. Rev. D **103**, L121301 (2021), arXiv:2012.11632 [hep-ph].
[59] Andrea Caputo, Georg Raffelt, and Edoardo Vitagliano, "Muonic boson limits: Supernova redux," Phys. Rev. D **105**, 035022 (2022), arXiv:2109.03244 [hep-ph].
[60] Andrea Caputo, Georg Raffelt, and Edoardo Vitagliano, "Radiative transfer in stars by feebly interacting bosons," JCAP **08**, 045 (2022), arXiv:2204.11862 [astro-ph.SR].
[61] Ricardo Z. Ferreira, M. C. David Marsh, and Eike Müller, "Strong supernovae bounds on ALPs from quantum loops," JCAP **11**, 057 (2022), arXiv:2205.07896 [hep-ph].
[62] Alessandro Lella, Pierluca Carenza, Giuseppe Lucente, Maurizio Giannotti, and Alessandro Mirizzi, "Protoneutron stars as cosmic factories for massive axionlike particles," Phys. Rev. D **107**, 103017 (2023), arXiv:2211.13760 [hep-ph].
[63] Alessandro Lella, Pierluca Carenza, Giampaolo Co', Giuseppe Lucente, Maurizio Giannotti, Alessandro Mirizzi, and Thomas Rauscher, "Getting the most on supernova axions," Phys. Rev. D **109**, 023001 (2024), arXiv:2306.01048 [hep-ph].
[64] Andrea Caputo and Georg Raffelt, "Astrophysical Axion Bounds: The 2024 Edition," PoS **COSMICWISPers**, 041 (2024), arXiv:2401.13728 [hep-ph].
[65] Alessandro Lella, Eike Ravensburg, Pierluca Carenza, and M. C. David Marsh, "Supernova limits on QCD axionlike particles," Phys. Rev. D **110**, 043019 (2024), arXiv:2405.00153 [hep-ph].
[66] Damiano F. G. Fiorillo, Tetyana Pitik, and Edoardo Vitagliano, "Supernova production of axion-like particles coupling to electrons, reloaded," (2025), arXiv:2503.15630 [hep-ph].
[67] Peter Sutherland, John N. Ng, Elliott Flowers, Malvin Ruderman, and Cullen Inman, "Astrophysical Limitations on Possible Tensor Contributions to Weak Neutral Current Interactions," Phys. Rev. D **13**, 2700 (1976).
[68] Duane A. Dicus and Edward W. Kolb, "Stellar Energy Loss Rates Due to S P T Neutral Currents," Phys. Rev. D **15**, 977 (1977).
[69] Riccardo Barbieri and Rabindra N. Mohapatra, "Limits on Right-handed Interactions From SN1987A Observations," Phys. Rev. D **39**, 1229 (1989).
[70] William DeRocco, Peter W. Graham, Daniel Kasen, Gustavo Marques-Tavares, and Surjeet Rajendran, "Supernova signals of light dark matter," Phys. Rev. D **100**, 075018 (2019), arXiv:1905.09284 [hep-ph].
[71] Claudio Andrea Manzari, Jorge Martin Camalich, Jonas Spinner, and Robert Ziegler, "Supernova limits on muonic dark forces," Phys. Rev. D **108**, 103020 (2023), arXiv:2307.03143 [hep-ph].
[72] Stefan Vogl and Xun-Jie Xu, "Heating the dark matter halo with dark radiation from supernovae," JCAP **07**, 058 (2025), arXiv:2411.18052 [hep-ph].
[73] P. S. Bhupal Dev, Doojin Kim, Deepak Sathyan, Kuver Sinha, and Yongchao Zhang, "New Constraints on Neutrino-Dark Matter Interactions: A Comprehensive Analysis," (2025), arXiv:2507.01000 [hep-ph].
[74] Koun Choi *et al.*, "New Physics Opportunities at Neutrino Facilities: BSM Physics at Accelerator, Atmospheric, and Reactor Neutrino Experiments," (2025), arXiv:2506.15306 [hep-ph].
[75] G. G. Raffelt, *Stars as laboratories for fundamental physics: The astrophysics of neutrinos, axions, and other weakly interacting particles* (1996).
[76] Shao-Feng Ge, Xiao-Gang He, Xiao-Dong Ma, and Jie Sheng, "Revisiting the fermionic dark matter absorption on electron target," JHEP **05**, 191 (2022), arXiv:2201.11497 [hep-ph].
[77] Dan Zhang *et al.* (PandaX), "Search for Light Fermionic Dark Matter Absorption on Electrons in PandaX-4T," Phys. Rev. Lett. **129**, 161804 (2022), arXiv:2206.02339 [hep-ex].
[78] Xinning Zeng *et al.* (PandaX), "Exploring New Physics with PandaX-4T Low Energy Electronic Recoil Data," Phys. Rev. Lett. **134**, 041001 (2025), arXiv:2408.07641 [hep-ex].
[79] J. X. Liu *et al.* (CDEX), "First Search for Light Fermionic Dark Matter Absorption on Electrons Using Germanium Detector in CDEX-10 Experiment," (2024), arXiv:2404.09793 [hep-ex].
[80] Robert Bollig, William DeRocco, Peter W. Graham, and Hans-Thomas Janka, "Muons in supernovae: implications for the axion-muon coupling," Phys. Rev. Lett. **125**, 051104 (2020), arXiv:2005.07141 [hep-ph].
[81] Yakov Borisovich Zel'dovich and Jurij P. Rajzer, *Physics of shock waves and high temperature hydrodynamic phenomena* (Academic Press, 1966-1968).
[82] Subrahmanyan Chandrasekhar, *An Introduction to the study of stellar structure* (Dover Publ., 1957).
[83] Steven Weinberg, *Lectures on astrophysics* (Cambridge University Press, 2020).
[84] Evan Frangipane, Stefania Gori, and Bibhushan Shakya, "Dark matter freeze-in with a heavy mediator: be-

yond the EFT approach," JHEP **09**, 083 (2022), arXiv:2110.10711 [hep-ph].
[85] Yugen Lin, Chih-Ting Lu, and Ningqiang Song, "Supernova cooling from neutrino-devouring dark matter," (2025), arXiv:2507.22124 [hep-ph].
[86] Benjamin V. Lehmann and Stefano Profumo, "Cosmology and prospects for sub-MeV dark matter in electron recoil experiments," Phys. Rev. D **102**, 023038 (2020), arXiv:2002.07809 [hep-ph].
[87] Lawrence J. Hall, Karsten Jedamzik, John March-Russell, and Stephen M. West, "Freeze-In Production of FIMP Dark Matter," JHEP **03**, 080 (2010), arXiv:0911.1120 [hep-ph].
[88] Francesco D'Eramo, Nicolas Fernandez, and Stefano Profumo, "Dark Matter Freeze-in Production in Fast-Expanding Universes," JCAP **02**, 046 (2018), arXiv:1712.07453 [hep-ph].
[89] Marcin Badziak, Keisuke Harigaya, Michał Łukawski, and Robert Ziegler, "Thermal production of astrophobic axions," JHEP **09**, 136 (2024), arXiv:2403.05621 [hep-ph].
[90] M. Kawasaki, Kazunori Kohri, and Naoshi Sugiyama, "MeV scale reheating temperature and thermalization of neutrino background," Phys. Rev. D **62**, 023506 (2000), arXiv:astro-ph/0002127.
[91] Steen Hannestad, "What is the lowest possible reheating temperature?" Phys. Rev. D **70**, 043506 (2004), arXiv:astro-ph/0403291.

Supplementary Material for The SN1987A Cooling Bound on Dark Matter Absorption in Electron Targets

Claudio Andrea Manzari, Jorge Martin Camalich, Jonas Spinner, and Robert Ziegler

CONTENTS

I. KINEMATICS IN CM AND PNS FRAMES

Here we discuss the setup for the production of DM in the PNS medium through the annihilation and scattering processes in Fig. 2. We choose a coordinate system where the 4-momenta of the incoming ψ_1 and ψ_2 particles in the PNS frame read

$$p_1 = (E_1, 0, 0, \bar{p}_1)\,, \qquad p_2 = (E_2, \bar{p}_2 s_\theta, 0, \bar{p}_2 c_\theta)\,, \tag{S1}$$

with $\bar{p}_i \equiv |\vec{p}_i| = \sqrt{E_i^2 - m_i^2}$ and $s_\theta = \sin\theta, c_\theta = \cos\theta$. In the center-of-mass (CM) frame the incoming ψ_1 and ψ_2 particles collide along the z-axis with 4-momenta

$$p_1' = (E_1', 0, 0, \bar{p}_{12}')\,, \qquad p_2' = (E_2', 0, 0, -\bar{p}_{12}')\,, \tag{S2}$$

where

$$\bar{p}_{12}' = \frac{1}{2\sqrt{s}}\lambda^{1/2}(s, m_1^2, m_2^2)\,, \qquad E_1' = \frac{1}{2\sqrt{s}}\left(s + m_1^2 - m_2^2\right)\,, \qquad E_2' = \frac{1}{2\sqrt{s}}\left(s - m_1^2 + m_2^2\right)\,, \tag{S3}$$

with $\lambda(a,b,c) = a^2 + b^2 + c^2 - 2(ab + ac + bc)$. The outgoing particles ψ_3 and χ scatter under a polar angle θ' with respect to the z-axis and within a plane $\mathcal{P}'$ that forms an azimuthal angle ϕ' with respect to the $x - z$ plane:

$$p_3' = (E_3', \bar{p}_{34}'\,(s_{\theta'}c_{\phi'}, s_{\theta'}s_{\phi'}, c_{\theta'}))\,, \qquad p_4' = (E_4', -\bar{p}_{34}'\,(s_{\theta'}c_{\phi'}, s_{\theta'}s_{\phi'}, c_{\theta'}))\,, \tag{S4}$$

where

$$\bar{p}_{34}' = \frac{1}{2\sqrt{s}}\lambda^{1/2}(s, m_3^2, m_\chi^2)\,, \qquad E_3' = \frac{1}{2\sqrt{s}}\left(s + m_3^2 - m_\chi^2\right)\,, \qquad E_4' = \frac{1}{2\sqrt{s}}\left(s - m_3^2 + m_\chi^2\right)\,. \tag{S5}$$

The Mandelstam variable t evaluated in in the CM frame can be written in terms of s and the polar angle θ',

$$t = (p_2 - p_4)^2 = -\frac{1}{2s}\left(s^2 + m_1^2 m_3^2 + m_2^2 m_\chi^2 - m_1^2 m_\chi^2 - m_2^2 m_3^2\right) + \frac{1}{2}\left(m_1^2 + m_2^2 + m_3^2 + m_\chi^2\right) + 2\,\bar{p}_{12}'\bar{p}_{34}' c_{\theta'}\,. \tag{S6}$$

The Lorentz transformation from the PNS frame to the CM frame is given by

$$\vec{\beta} = \frac{\bar{p}}{E}(s_\eta, 0, c_\eta)\,, \qquad\qquad \gamma = \frac{E}{\sqrt{s}}\,, \tag{S7}$$

where we have defined

$$E = E_1 + E_2\,, \qquad\qquad \bar{p} = |\vec{p}_1 + \vec{p}_2| = \sqrt{E^2 - s}\,, \tag{S8}$$

with the angle η given by

$$c_\eta = \frac{\sqrt{s}E_1 - EE_1'}{\bar{p}\bar{p}_{12}'}\,. \tag{S9}$$

This relation allows the final state energies in the PNS frame to be expressed in terms of the kinematic variables as

$$E_3 = \frac{1}{\sqrt{s}}\left(EE_3' + \bar{p}\bar{p}_{34}'\left(s_{\theta'}c_{\phi'}s_\eta + c_{\theta'}c_\eta\right)\right)\,, \qquad\qquad E_4 = \frac{1}{\sqrt{s}}\left(EE_4' - \bar{p}\bar{p}_{34}'\left(s_{\theta'}c_{\phi'}s_\eta + c_{\theta'}c_\eta\right)\right)\,. \tag{S10}$$

With these definitions, one obtains Eqs. (4) and (14).

II. SCATTERING AMPLITUDES, CROSS-SECTIONS, COOLING RATES

Here we provide results for squared matrix elements, cross-sections and the approximate cooling rates for general effective operators defined by (note that only one tensor operator is independent)

$$\mathcal{L}_\chi = \frac{1}{\Lambda_V^2}(\bar{e}\gamma^\mu e)(\bar{\chi}\gamma_\mu\nu_L) + \frac{1}{\Lambda_A^2}(\bar{e}\gamma^\mu\gamma_5 e)(\bar{\chi}\gamma_\mu\nu_L) + \frac{1}{\Lambda_S^2}(\bar{e}e)(\bar{\chi}\nu_L) + \frac{1}{\Lambda_P^2}(\bar{e}\gamma_5 e)(\bar{\chi}\nu_L) + \frac{1}{\Lambda_T^2}(\bar{e}\sigma^{\mu\nu}e)(\bar{\chi}\sigma_{\mu\nu}\nu_L) + \text{h.c.} \tag{S11}$$

We will first discuss annihilation processes and then scattering, turning on a single operator in Eq. (S11) at a time.

II.a. Annihilation

The spin-summed (but not spin-averaged) squared matrix elements for annihilation processes $e^+e^- \to \chi\overline{\nu}$ and $e^+e^- \to \overline{\chi}\nu$ are given by

$$\sum_{\text{spins}} |\mathcal{M}_{\text{an}}^V|^2 = \frac{4}{\Lambda_V^4}\left(2m_e^4 - 4m_e^2 t + 2t\left(s + t - m_\chi^2\right) + s\left(s - m_\chi^2\right)\right)\,, \tag{S12}$$

$$\sum_{\text{spins}} |\mathcal{M}_{\text{an}}^A|^2 = \frac{4}{\Lambda_A^4}\left(2m_e^4 + 4m_e^2(m_\chi^2 - s - t) - m_\chi^2(s + 2t) + s^2 + 2\,s\,t + 2\,t^2\right)\,, \tag{S13}$$

$$\sum_{\text{spins}} |\mathcal{M}_{\text{an}}^S|^2 = \frac{2}{\Lambda_S^4}(s - 4m_e^2)(s - m_\chi^2)\,, \tag{S14}$$

$$\sum_{\text{spins}} |\mathcal{M}_{\text{an}}^P|^2 = \frac{2}{\Lambda_P^4}s(s - m_\chi^2)\,, \tag{S15}$$

$$\sum_{\text{spins}} |\mathcal{M}_{\text{an}}^T|^2 = \frac{16}{\Lambda_T^4}\left(4m_e^2 + 2m_e^2(m_\chi^2 - s - 4t) - m_\chi^2(s + 4t) + (s + 2t)^2\right)\,, \tag{S16}$$

with the Mandelstam variables

$$s = 2m_e^2 + 2(E_1E_2 - \bar{p}_1\bar{p}_2c_\theta)\,, \qquad t = (p_{e^-} - p_{\chi(\overline{\chi})})^2 = m_e^2 - \frac{s - m_\chi^2}{2}\left(1 - \beta_e\,c_{\theta'}\right)\,, \qquad \beta_e = \sqrt{1 - \frac{4m_e^2}{s}}\,, \tag{S17}$$

and θ' (θ) are the scattering angles in the CM (PNS) frame, see SupM I. The corresponding cross-sections read

$$\sigma^V_{e^+e^-\to\chi\overline{\nu}} = \frac{\beta_e}{48\pi\Lambda_V^4 s^2(s-4m_e^2)}(s+2m_e^2)(s-m_\chi^2)^2(2s+m_\chi^2)\,, \tag{S18}$$

$$\sigma^A_{e^+e^-\to\chi\overline{\nu}} = \frac{\beta_e}{48\pi\Lambda_A^4 s^2(s-4m_e^2)}(s-m_\chi^2)^2\left(s(2s+m_\chi^2)+2m_e^2(m_\chi^2-4s)\right)\,, \tag{S19}$$

$$\sigma^S_{e^+e^-\to\chi\overline{\nu}} = \frac{\beta_e}{32\pi\Lambda_S^4 s}(s-m_\chi^2)^2\,, \tag{S20}$$

$$\sigma^P_{e^+e^-\to\chi\overline{\nu}} = \frac{\beta_e}{32\pi\Lambda_P^4 (s-4m_e^2)}(s-m_\chi^2)^2\,, \tag{S21}$$

$$\sigma^T_{e^+e^-\to\chi\overline{\nu}} = \frac{\beta_e}{12\pi\Lambda_T^4 s^2(s-4m_e^2)}(s+2m_e^2)(s-m_\chi^2)^2(s+2m_\chi^2)\,, \tag{S22}$$

and the inverse processes can be obtained using the relation

$$\sigma^X_{\chi\overline{\nu}\to e^+e^-} = \frac{4s(s-4m_e^2)}{\mathfrak{g}_\chi(s-m_\chi^2)^2}\sigma^X_{e^+e^-\to\chi\overline{\nu}}\,, \tag{S23}$$

for $X = V, A, P, S, T$ and g_χ denotes the number of degrees of freedom in χ. Employing the approximation $(1-f_3)\to F_{\overline{\nu}}$ (for $e^+e^-\to\chi\overline{\nu}$), one can easily calculate $J^X_{s,\rm ann}$ using Eq. (4) as the integrals ϕ' and c'_θ are trivial. Taking the massless limit, $m_e = m_\chi = 0$, gives

$$J^X_{s,\rm an} = s^2\frac{E_1+E_2}{6\pi\Lambda_X^4}a_X F_{\overline{\nu}}\,, \tag{S24}$$

where $a_V = a_A = 4a_S/3 = 4a_P/3 = a_T/2 = 1$. The analogous expressions for $e^+e^-\to\overline{\chi}\nu$ are identical except for the Pauli blocking factor $(1-f_3)$ that instead contains the chemical potential of the neutrino and becomes F_ν with our approximations. This leads to

$$Q^X_{\rm an} = \frac{a_X T^9 F_{\nu(\overline{\nu})}}{18\pi^5\Lambda_X^4}H_4(y_e)H_3(-y_e) + (y_e\to -y_e)\,, \tag{S25}$$

where $y_i = \mu_i/T$ and using Eq. (7). Likewise, the absorption width and rates for the process $\chi\bar{\nu}\to e^+e^-$, in the $m_e = m_\chi = 0$ limit, are

$$K^X_{\rm an} = \frac{s^2}{3\pi\Lambda_X^4}a_X F_e F_{\bar{e}}\,, \tag{S26}$$

$$\Gamma^X_{\rm an} = \frac{2E_\chi T^4 H_3(-y_\nu)}{9\,\mathfrak{g}_\chi\pi^3\Lambda_X^4}a_X F_e F_{\bar{e}}\,, \tag{S27}$$

$$\mathcal{C}^X_{\rm an} = \frac{T^8 H_3(-y_\nu)H_3(y_\nu)}{9\pi^5\Lambda_X^4}a_X F_e F_{\bar{e}}\,, \tag{S28}$$

where we have defined the collision operator,

$$\mathcal{C} = \mathfrak{g}_\chi\int\frac{d^3\vec{p}_\chi}{(2\pi)^3}f_\chi\Gamma(E_\chi). \tag{S29}$$

II.b. Scattering

The spin-summed (but not spin-averaged) squared matrix elements for scattering processes $e^{\mp}\nu \to e^{\mp}\chi$ or $e^{\mp}\bar{\nu} \to e^{\mp}\bar{\chi}$ are given by

$$\begin{aligned}
\sum |\mathcal{M}^V_{\rm sc}|^2 =& \frac{4}{\Lambda_V^4}\left(2s^2+2st+t^2-2m_e^2\left(2s-m_e^2\right)-m_\chi^2(2s+t)\right)\,,\\
\sum |\mathcal{M}^A_{\rm sc}|^2 =& \frac{4}{\Lambda_A^4}\left(4m_e^2\left(m_\chi^2-s-t\right)+2m_e^4-m_\chi^2(2s+t)+2s^2+2st+t^2\right)\,,\\
\sum |\mathcal{M}^S_{\rm sc}|^2 =& \frac{2}{\Lambda_S^4}\left(t-4m_e^2\right)\left(t-m_\chi^2\right)\,,\\
\sum |\mathcal{M}^P_{\rm sc}|^2 =& \frac{2}{\Lambda_P^4}t\left(t-m_\chi^2\right)\,,\\
\sum |\mathcal{M}^T_{\rm sc}|^2 =& \frac{16}{\Lambda_T^4}\left(2m_e^2\left(m_\chi^2-4s-t\right)+4m_e^4-m_\chi^2(4s+t)+(2s+t)^2\right)\,,
\end{aligned} \tag{S30}$$

with the Mandelstam variable

$$t=\frac{m_\chi^2}{2}\left(1+\frac{m_e^2}{s}\right)-\frac{s-m_e^2}{2}\left(1-\frac{m_e^2}{s}-\beta_{e\chi}c_{\theta'}\right)\,,\qquad \beta_{e\chi}=\sqrt{1-2\frac{m_e^2+m_\chi^2}{s}+\frac{(m_e^2-m_\chi^2)^2}{s^2}}\,, \tag{S31}$$

and θ' is the scattering angle in the CM frame, see SupM I. The corresponding cross-sections read

$$\begin{aligned}
\sigma^V_{e^{\mp}\nu\to e^{\mp}\chi} &= \frac{\beta_{e\chi}}{48\pi\Lambda_V^4 s^2}\left(8s^3-s^2(12m_e^2+7m_\chi^2)-s(m_\chi^4-6m_e^4+3m_e^2m_\chi^2)-2m_e^2(m_e^2-m_\chi^2)^2\right)\,,\\
\sigma^A_{e^{\mp}\nu\to e^{\mp}\chi} &= \frac{\beta_{e\chi}}{48\pi\Lambda_A^4 s^2}\left(8s^3-7m_\chi^2s^2-s(m_\chi^4+6m_e^4-9m_e^2m_\chi^2)-2m_e^2(m_e^2-m_\chi^2)^2\right)\,,\\
\sigma^S_{e^{\mp}\nu\to e^{\mp}\chi} &= \frac{\beta_{e\chi}}{96\pi\Lambda_S^4 s^2}\left(2s^3-s^2(m_\chi^2-6m_e^2)-s(6m_e^4+m_\chi^4-9m_e^2m_\chi^2)-2m_e^2(m_e^2-m_\chi^2)^2\right)\,,\\
\sigma^P_{e^{\mp}\nu\to e^{\mp}\chi} &= \frac{\beta_{e\chi}}{96\pi\Lambda_P^4 s^2}\left(2s^3-s^2(6m_e^2+m_\chi^2)-s(m_\chi^4-6m_e^4+3m_e^2m_\chi^2)-2m_e^2(m_e^2-m_\chi^2)^2\right)\,,\\
\sigma^T_{e^{\mp}\nu\to e^{\mp}\chi} &= \frac{\beta_{e\chi}}{12\pi\Lambda_T^4 s^2}\left(14s^3-s^2(12m_e^2+13m_\chi^2)-sm_\chi^2(m_\chi^2-3m_e^2)-2m_e^2(m_e^2-m_\chi^2)^2\right)\,,
\end{aligned} \tag{S32}$$

and the inverse processes can be obtained using the relation

$$\sigma^X_{e^{\mp}\chi\to e^{\mp}\nu}=\frac{1}{\mathfrak{g}_\chi}\frac{(s-m_e^2)^2}{s^2-2s(m_e^2+m_\chi^2)+(m_e^2-m_\chi^2)^2}\sigma^X_{e^{\mp}\nu\to e^{\mp}\chi}\,. \tag{S33}$$

Using the approximation $(1-f_3)\to F_{e^\pm}$ (F_{e^-} for $e^-\nu\to e^-\chi$ and $e^-\bar{\nu}\to e^-\bar{\chi}$ and F_{e^+} for $e^+\nu\to e^+\chi$ and $e^+\bar{\nu}\to e^+\bar{\chi}$)), with $E_1=E_{e^\pm}, E_2=E_{\nu/\bar{\nu}}$, and taking the massless limits, $m_e=m_\chi=0$, we obtain

$$J^{V,A}_{s,\rm sc}=\frac{s^2}{24\pi\Lambda^4_{V,A}}(7E_1+9E_2)F_{e^\pm}\,, \tag{S34}$$

$$\hat{J}^{S,P}_{s,\rm sc}=\frac{s^2}{48\pi\Lambda^4_{S,P}}(3E_1+E_2)F_{e^\pm}\,, \tag{S35}$$

$$J^{T}_{s,\rm sc}=\frac{s^2}{6\pi\Lambda^4_{T}}(11E_1+17E_2)F_{e^\pm}\,, \tag{S36}$$

which permits to analytically solve the final integrals to calculate the energy loss rates in this limit for $e^-\nu\to e^-\chi$:

$$\begin{aligned}
Q^{V,A}_{\rm sc} &= \frac{T^9F_{e^-}}{72\pi^5\Lambda^4_{V,A}}\left[7H_4(y_e)H_3(y_\nu)+9H_4(y_\nu)H_3(y_e)\right]\,,\\
Q^{S,P}_{\rm sc} &= \frac{T^9F_{e^-}}{144\pi^5\Lambda^4_{S,P}}\left(3H_4(y_e)H_3(y_\nu)+H_4(y_\nu)H_3(y_e)\right)\,,\\
Q^{T}_{\rm sc} &= \frac{T^9F_{e^-}}{18\pi^5\Lambda^4_{T}}\left(11H_4(y_e)H_3(y_\nu)+17H_4(y_\nu)H_3(y_e)\right)\,.
\end{aligned} \tag{S37}$$

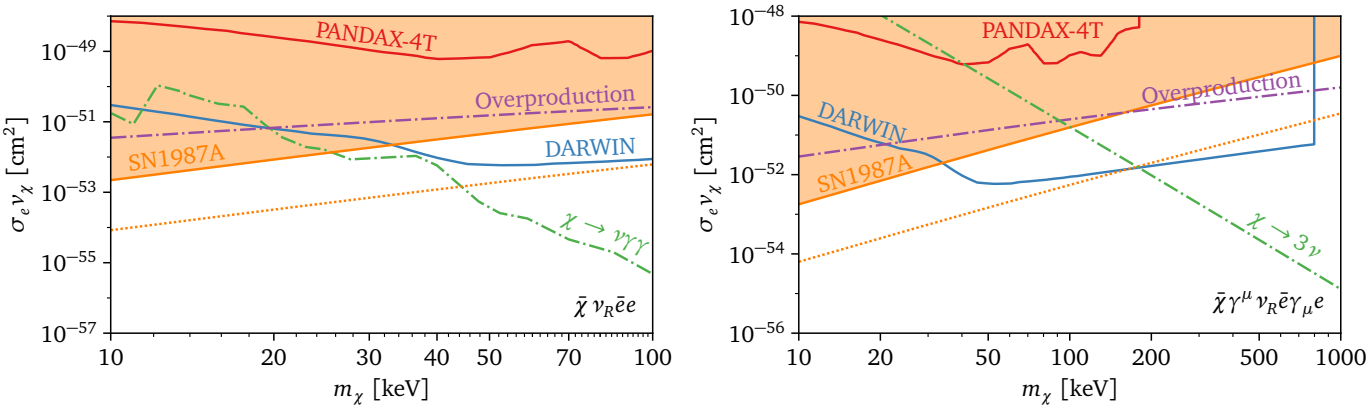

FIG. S1. SN 1987A cooling bound for scalar (left) and vector (right) interactions and sterile neutrinos. See caption of Fig. 1.

Other channels like $e^-\bar{\nu} \to e^-\bar{\chi}$ or $e^+\nu \to e^+\chi$ are obtained from Eq. (8) by replacing the arguments of the $H_n(y)$ functions accordingly. However, the scattering contributions in Eq. (S37) give the dominant contributions to the total energy-loss rate, and result in the final lower bounds on the UV scales in the free-streaming regime, given by

$$\Lambda_X \gtrsim \begin{cases} (15-22)\ \text{TeV} & X = V, A \\ (9.3-14)\ \text{TeV} & X = S, P \\ (25-37)\ \text{TeV} & X = T \end{cases} . \tag{S38}$$

where the lower (upper) value corresponds to the SFHo18.80 (SFHo20.0) simulation.

$$K^X_{s,\text{sc}} = \frac{2s^2}{3\pi\Lambda_X^4} d_X F_e F_\nu \,, \tag{S39}$$

$$\Gamma^X_{s,\text{sc}} = \frac{4E_\chi T^4 H_3(y_e)}{9\,\mathfrak{g}_\chi \pi^3 \Lambda_X^4} d_X F_e F_\nu \,, \tag{S40}$$

$$\mathcal{C}^X_{s,\text{sc}} = \frac{2T^8 H_3(y_\nu) H_3(y_e)}{9\,\pi^5 \Lambda_X^4} d_X F_e F_\nu \,, \tag{S41}$$

with $d_{V,A} = 8\, d_{S,P} = d_T/7 = 1$. The trapping bounds are

$$\Lambda_X \gtrsim \begin{cases} (56-59)\ \text{GeV} & X = V, A \\ (38-41)\ \text{GeV} & X = S, P \\ (88-92)\ \text{GeV} & X = T \end{cases} , \tag{S42}$$

covering the range obtained using the simulations SFHo18.80 or SFHo20.0.

II.c. Effective operators with sterile neutrinos

Another possibility that has been considered for absorption signatures in DD is to replace the SM neutrino by a sterile one in the effective Lagrangian (S11) with $m_\nu \ll m_\chi$ [48] . In the context of the DM production in SNe, these models are substantially different from the ones considered with SM neutrinos. In the former case, the most important production mechanism is scattering $\nu_L e^- \to \chi e^-$, where SM neutrinos are in thermal equilibrium with the plasma. However, sterile neutrinos are not in equilibrium and the only possible production mechanism is annihilation, $e^-e^+ \to \chi\bar{\nu}_R$ and $e^-e^+ \to \bar{\chi}\nu_R$. In fact, this is similar to the production of DM in SN with $(\bar{e}e)\,(\bar{\chi}\chi)$ interactions studied in Ref. [71], although in this case the emission of both χ and ν_R contributes to cooling.

In Fig. S1, we present the SN upper limits on DD cross sections, using the same style as in Fig. 1. These bounds are significantly weaker than those obtained for SM neutrinos, but are still complementary to both ID and DD. However, some parameter space remains accessible to DD searches for vector interactions, particularly within the region where the SN constraints are subject to uncertainties.

III. LIGHT MEDIATORS

We will investigate here the extension of the SN 1987A limits that we have derived in the EFT limit to the case where $(\overline{\nu}\chi)(\overline{e}e)$ interactions are produced by *light* mediators, with mass $M \lesssim 100$ MeV. In this case, mediators can be produced on-shell (resonantly) enhancing the efficiency of the dark production and absorption processes. For simplicity, in the following we focus on the massless approximations for electrons and dark particles χ. Let us discuss the main contributions to the production and absorption resonant processes.

III.a. Annihilation

Resonant production of χ through $e^+e^- \to X^* \to \chi\bar{\nu}$ occurs as long as the collision energies of the positrons and electrons in the plasma are sufficiently large, i.e. $m_X \lesssim 3T$. In this regime and taking the limit $m_\chi = m_e \to 0$, we obtain

$$J_s = 2\,C_X s^2 \frac{(E_1+E_2) g_e^2 \mathrm{BR}_\chi}{m_X} F_{\bar{\nu}} \frac{\Gamma_X}{(s-m_X^2)^2 + m_X^2\Gamma_X^2}, \tag{S43}$$

where $C_V = C_A = 2\,C_S = 2\,C_P = 1$, $\mathrm{BR}_\chi = \Gamma(X \to \chi\bar{\nu})/\Gamma_X$ is the branching fraction of X into the dark channel $\chi\bar{\nu}$, and $\Gamma(X \to \chi\bar{\nu}) = A_X g_\chi^2 m_X/12\pi$, with $A_V = 2\,A_S/3 = 1$, and g_i the couplings of the mediator to fermion i. Assuming $\Gamma_X/m_X \ll 1$ one can apply the narrow-width approximation (NWA), and obtain

$$J_s = 2\,C_X \pi m_X^2 (E_1+E_2) g_e^2 \mathrm{BR}_\chi F_{\bar{\nu}} \delta(s-m_X^2), \tag{S44}$$

and

$$Q = C_X \frac{g_e^2 m_X^2 \mathrm{BR}_\chi T^3}{32\pi^3} F_{\bar{\nu}} \left(H_1(y_e)H_0(-y_e) + H_1(-y_e)H_0(y_e)\right). \tag{S45}$$

One can also explicitly solve the full phase-space integrals with the resonant structure (beyond NWA) finding a good description of the production process below $m_X \simeq 100$ MeV for the benchmark SN conditions.

Likewise, one can adapt the calculation of the absorption width and rates of the process $\chi\bar{\nu} \to X^* \to e^+e^-$ to the light-mediator regime,

$$K_s = 4\,C_X\, s^2 \frac{g_e^2 \mathrm{BR}_\chi}{m_X} F_e F_{\bar{e}} \frac{\Gamma_V}{(s-m_X^2)^2 + m_X^2\Gamma_X^2}\,, \tag{S46}$$

and in the NWA,

$$K_s = 4\,C_X\, \pi m_X^2 g_e^2 \mathrm{BR}_\chi F_e F_{\bar{e}} \delta(s-m_X^2)\,. \tag{S47}$$

In this limit we obtain,

$$\Gamma_{\mathrm{an}}(E_\chi) = C_X \frac{g_e^2 m_X^2 T}{8\pi E_\chi^2 \mathfrak{g}_\chi} \mathrm{BR}_\chi F_e F_{\bar{e}} \log\left(1+e^{-y_\nu}\right), \tag{S48}$$

and

$$\mathcal{C}_{\mathrm{abs}} = C_X \frac{g_e^2 m_X^2 T^2}{16\pi^3} \mathrm{BR}_\chi F_e F_{\bar{e}} \log\left(1+e^{-y_\nu}\right) \log\left(1+e^{y_\nu}\right). \tag{S49}$$

III.b. Scattering

Scattering processes like $e^-\nu \to e^-\chi$ arise by t-channel exchange of the X mediator. Although this process does not suffer from the suppression of the positron abundance in the plasma (see discussion in the EFT), it scales with the coupling constant as $\propto g^4$, compared to the $\propto g^2$ scaling of resonant annihilation in the light mediator regime. Thus,

it is expected that for the small couplings required by the SN 1987A bound, the latter will dominate the emission and absorption rates. In this regime, for a vector mediator, we obtain

$$J_s^{A,V} = \frac{g_e^2 g_\chi^2}{4\pi s^2} F_{e^-} \left(2\log\left(\frac{s}{m_X^2}+1\right)\left(3m_X^4(E_1-E_2)+2m_X^2 s(2E_1-3E_2)+2s^2(E_1-2E_2)\right) \right.$$
$$\left. - \frac{E_1 s\left(6m_X^4+11m_X^2 s+7s^2\right)}{m_X^2+s} + E_2 s\left(\frac{4s^2}{m_X^2}+6m_X^2+9s\right)\right). \tag{S50}$$

while for a scalar mediator,

$$J_s^{S,P} = \frac{g_e^2 g_\chi^2}{16\pi s^2} F_{e^-} \left(2\log\left(\frac{s}{m_S^2}+1\right)\left(3m_S^4(E_1-E_2)-2E_2 s\, m_S^2\right) + E_1 s\left(-4m_S^2+s-\frac{2m_S^4}{m_S^2+s}\right) + E_2 s(s+6m_S^2)\right). \tag{S51}$$

A significant simplification can be achieved for light mediators expanding the previous formulae in m_V and m_S around zero,

$$J_s^{V,A} = \frac{g_\chi^2 g_e^2 E_2 s}{\pi m_V^2} F_{e^-}\,, \qquad J_s^{S,P} = \frac{g_\chi^2 g_e^2 (E_1+E_2)}{16\pi} F_{e^-}\,. \tag{S52}$$

In this limit, one finally gets

$$Q^{V,A} = \frac{g_\chi^2 g_e^2 T^7}{8\pi^5 m_V^2} F_{e^-} H_2(y_e) H_3(y_\nu)\,, \qquad Q^{S,P} = \frac{g_\chi^2 g_e^2 T^5}{256\pi^5} F_{e^-}(H_2(y_e)H_1(y_\nu)+H_1(y_e)H_2(y_\nu)). \tag{S53}$$

The calculation of the absorption rate for the inverse scattering process yields

$$K_s^{V,A} = \frac{g_e^2 g_\chi^2}{2\pi} F_e F_\nu \left(\frac{m_V^2}{m_V^2+s} + \frac{2s}{m_V^2} + \frac{2\left(m_V^2+s\right)\log\left(\frac{m_V^2}{m_V^2+s}\right)}{s} + 1 \right)\,,$$
$$K_s^{S,P} = \frac{g_e^2 g_\chi^2}{4\pi\, s} F_e F_\nu \left(\frac{2\,s\,m_S^2+s^2}{m_S^2+s} + 2m_S^2 \log\left(\frac{m_S^2}{m_S^2+s}\right)\right)\,. \tag{S54}$$

In the limit $m_V, m_S \to 0$ one obtains $K_s^{V,A} = g_e^2 g_\chi^2 s F_e F_\nu/\pi m_V^2$, $K_s^{S,P} = g_e^2 g_\chi^2 F_e F_\nu/(4\pi)$ and

$$\Gamma_{\rm sc}^{V,A}(E_\chi) = \frac{g_e^2 g_\chi^2 T^3}{4\pi^3 m_V^2 \mathfrak{g}_\chi} F_e F_\nu H_2(y_e), \qquad \mathcal{C}_{\rm sc}^{V,A} = \frac{g_e^2 g_\chi^2 T^6}{8\pi^5 m_V^2} F_e F_\nu H_2(y_e) H_2(y_\nu)\,,$$
$$\Gamma_{\rm sc}^{S,P}(E_\chi) = \frac{g_e^2 g_\chi^2 T^2}{32\pi^3 E_\chi \mathfrak{g}_\chi} F_e F_\nu H_1(y_e), \qquad \mathcal{C}_{\rm sc}^{S,P} = \frac{g_e^2 g_\chi^2 T^4}{64\pi^5} F_e F_\nu H_1(y_e) H_1(y_\nu). \tag{S55}$$

III.c. Photoproduction

Photoproduction off electrons, $\gamma e^- \to V^*(\to \chi\bar{\nu})e^-$ is negligible compared to annihilation and scattering for heavy mediators but needs to be considered for light mediators [71]. We start with the volume emission rate, that will be approximated in the relativistic limit of electrons as [71],

$$Q_\gamma = \frac{F_{e^-}}{12\pi^4} \int_0^\infty d\omega\omega f_\gamma \int_0^\infty d\omega'\omega'(\omega+\omega') f_e \int_{-1}^{+1} d(\cos\theta) s\sigma(s)\,, \tag{S56}$$

where ω (ω') is the photon (electron) energy, $\sigma(s)$ is the photoproduction cross section, $s = 2\omega\omega'(1-\cos\theta)$ and we have assumed that the χ in the process carries away $\approx 1/3$ of the total energy in the collision. Given that this process is relevant only for light mediator masses, where the mediator X is produced resonantly, we use the NWA.

For a vector mediator the proper cross section for $e^-\gamma \to V e^-$ was obtained in Eq. (39) of Ref. [71]. For the scalar mediator in Eq. (17) one obtains

$$\sigma(\gamma e \to \phi e) = \frac{s^2 e^2 y_e^2}{16\pi\left(s-m_e^2\right)^3}\left[\left(1-\frac{2m_\phi^2}{s}+\frac{6m_e^2}{s}+\frac{9m_e^4}{s^2}-\frac{10m_\phi^2 m_e^2}{s^2}+\frac{2m_\phi^4}{s^2}\right)\log\left(\frac{1+(m_e^2-m_\phi^2)/s+\beta_f}{1+(m_e^2-m_\phi^2)/s-\beta_f}\right)\right.$$
$$\left. -\frac{\beta_f}{2}\left(3-\frac{7m_\phi^2}{s}+\frac{25m_e^2}{s}+\frac{5m_e^4}{s^2}-\frac{2m_e^2 m_\phi^2}{s^2}+\frac{m_e^4 m_\phi^2}{s^3}-\frac{m_e^6}{s^3}\right)\right] \tag{S57}$$

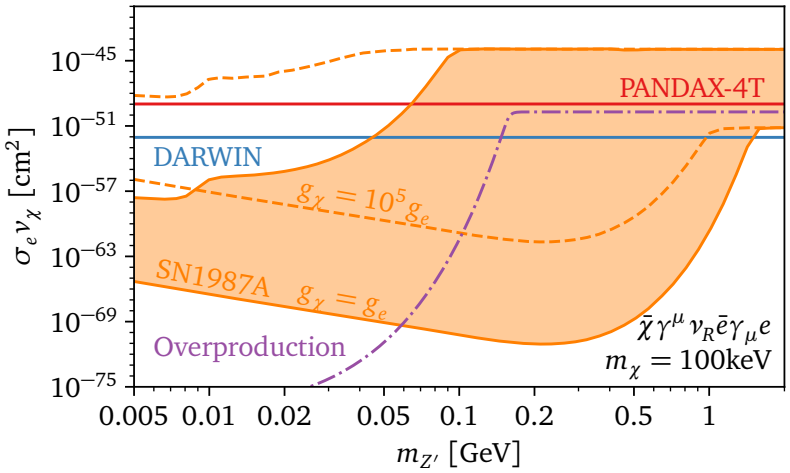

FIG. S2. Bounds on the DD cross-section for the absorption of DM with $m_\chi = 100$ keV, a sub-GeV vector mediator and a sterile neutrino. See caption of Fig. 3.

with $\beta_f = \sqrt{(1 - m_\phi^2/s)^2 - 2m_e^2/s(1 + m_\phi^2/s) + m_e^4/s^2}$.

III.d. Application to a simplified vector model coupled to sterile neutrinos

In the main article we discussed the importance of considering carefully the light-mediator regime when studying the SN bounds on sub-MeV DM models. The reason is the onset of resonant processes that change the dependence of the bounds in the couplings. We studied this for the scalar $(\bar{e}e)(\bar{\nu}\chi)$ interactions in Fig. 3. Here, we repeat the analysis for a simplified vectorial model featuring interactions with a sterile neutrino (instead of a SM one) [48],

$$\mathcal{L}_V \supset (g_\chi \bar{\chi}\gamma^\mu \nu_R + g_e \bar{e}\gamma^\mu e)\, Z'_\mu. \tag{S58}$$

As discussed above, in case of sterile neutrinos the calculations are analogous to those for the $(\bar{e}e)\,(\bar{\chi}\chi)$ interactions studied in Ref. [71]. Following this reference, in Fig. S2 we show the dependence of the bounds as a function of the mediator mass $m_{Z'}$ for a DM mass $m_\chi = 100$ keV. As in the scalar case represented in Fig. 3, the SN bounds become much stronger for light Z' opening up a region of cross sections that could be probed by DD. However, as in the case of the scalar mediator, cosmological production also becomes resonant, further constraining the allowed parameter space.

IV. OVERPRODUCTION LIMIT

In this section we discuss the limits from DM overproduction in both the EFT regime (the operators in Eq. (1)) and the scalar and vector UV completions in Eq. (17) and Eq. (S58), respectively. We follow Ref. [86] and integrate the Boltzmann equation in the freeze-in regime [87], see the appendices in Refs. [88, 89] for details. For the effective operators, the freeze-in contribution to the DM abundance is UV dominated, so that the abundance will grow with the reheating temperature T_R and decrease with the EFT scale Λ. In order to derive conservative lower bounds on Λ from DM overproduction, we thus assume the lowest possible reheating temperature $T_R = 4\,\text{MeV}$ [90, 91] and take a vanishing initial DM abundance (any non-zero abundance would make the limit stronger).

IV.a. General Case

For a general $2 \to 2$ process $\chi + 1 \to 2 + 3$ involving a single DM particle χ and particles 2 and 3 in the thermal bath, the Boltzmann Equation (BE) for the DM yield $Y_\chi \equiv n_\chi/s$ is given by

$$\begin{aligned}\frac{dY_\chi}{dT} &= -\frac{1}{sHT}\left(1 + \frac{dg_{*s}}{dT}\frac{T}{3g_{*s}}\right)\left[-\langle\sigma_{\chi 1\to 23}v\rangle n_\chi n_1 + \langle\sigma_{23\to\chi 1}v\rangle n_2^{\rm eq} n_3^{\rm eq}\right] \\ &= -\frac{1}{sHT}\left(1 + \frac{dg_{*s}}{dT}\frac{T}{3g_{*s}}\right)\langle\sigma_{\chi 1\to 23}v\rangle\left[n_\chi^{\rm eq} n_1^{\rm eq} - n_\chi n_1\right] \\ &= -\frac{1}{sHT}\left(1 + \frac{dg_{*s}}{dT}\frac{T}{3g_{*s}}\right)\mathcal{C}_{\chi 123}\left[1 - Y_\chi Y_1/(Y_\chi^{\rm eq} Y_1^{\rm eq})\right]\,, \end{aligned} \tag{S59}$$

with the collision operator $\mathcal{C}_{\chi 123} = \langle\sigma_{\chi 1\to 23}v\rangle n_\chi^{\rm eq} n_1^{\rm eq} = \langle\sigma_{23\to\chi 1}v\rangle n_2^{\rm eq} n_3^{\rm eq}$. It is convenient to introduce a reference scale m by defining $T = m/x$, so that the BE becomes

$$\frac{dY_\chi}{dx} = \frac{1}{sHx}\left(1 - \frac{dg_{*s}}{dx}\frac{x}{3g_{*s}}\right)\mathcal{C}_{\chi 123}\left[1 - Y_\chi Y_1/(Y_\chi^{\rm eq} Y_1^{\rm eq})\right]\,. \tag{S60}$$

Taking the effective degrees of freedom g_* to be approximately constant, one has $s \propto T^3, H \propto T^2$, and the BE simplifies to

$$\frac{dY_\chi(x)}{dx} = \frac{x^4\mathcal{C}_{\chi 123}(x)}{s(m)H(m)}\left[1 - Y_\chi(x)Y_1(x)/(Y_\chi^{\rm eq}(x)Y_1^{\rm eq}(x))\right]\,. \tag{S61}$$

In the present scenario it is clear that DM production continues at most until $T \approx m_e$, when the electrons become non-relativistic, so that $Y_1(x) \lesssim Y_1^{\rm eq(x)}$ for $1 = \nu, e$. Moreover in the freeze-in limit the DM abundance never reaches equilibrium, $Y_\chi \ll Y_\chi^{\rm eq}$, so that one can neglect the whole bracket on the RHS in Eq. (S61) to good approximation. We can then integrate both sides easily from the maximal temperature T_R with vanishing yield down to $T = 0$ for the asymptotic yield. More appropriate would be to integrate until the temperature where both electrons and neutrinos $T \approx 1\,\text{MeV}$, where both electrons and neutrinos have decoupled from the thermal path and electrons start to become non-relativistic, but in practice this difference does not matter much, as the integral is UV dominated and the IR boundary gives only a small correction. We thus obtain for the asymptotic yield Y_∞

$$Y_\infty \approx \int_{m/T_R}^{\infty}\frac{x^4\mathcal{C}_{\chi 123}(x)}{s(m)H(m)}\,dx = \frac{135\sqrt{5}M_{\rm Pl}}{4m^5\pi^{7/2}g_*^{3/2}(m)}\int_{m/T_R}^{\infty}x^4\mathcal{C}_{\chi 123}(x)\,dx \equiv R(m)\,. \tag{S62}$$

Including a factor 2 for the abundance for $Y_{\overline{\chi}}$ we finally get for the total relic abundance

$$\Omega_\chi h^2 \approx 2R(m)m_\chi s_0/\rho_{\rm crit} = 0.12\left(\frac{m_\chi}{10\,\text{keV}}\right)\left(\frac{R(m)}{2.2\times 10^{-5}}\right)\,. \tag{S63}$$

IV.b. Effective Operators

To calculate the relic abundance for the EFT operators in Eq. (1), we merely need to integrate the collision term. For simplicity we will work in the high-energy limit and neglect m_e and m_χ, in which case the collision terms for annihilation $e^+e^- \to \chi\overline{\nu}$ and scattering $e^\pm\nu \to e^\pm\chi$ are given in Eq. (S28) and Eq. (S41), respectively, in the limit of vanishing chemical potentials. Also taking the Boltzmannian limit for simplicity, we obtain

$$\hat{\mathcal{C}}_{e^+e^-\to\chi\overline{\nu}} = \frac{4a_X T^8}{\pi^5\Lambda_X^4}\,, \qquad \hat{\mathcal{C}}_{e^\pm\nu\to e^\pm\chi} = \frac{8d_X T^8}{\pi^5\Lambda_X^4}\,, \tag{S64}$$

where a_X and d_X are given below Eq. (S24) and Eq. (S41), respectively. The collision operator can be easily integrated, giving for annihilation

$$\int_{m/T_R}^{\infty}x^4\mathcal{C}_{e^+e^-\to\chi\overline{\nu}}(x)\,dx = \frac{4a_X m^8}{\pi^5\Lambda_X^4}\int_{m/T_R}^{\infty}\frac{dx}{x^4} = \frac{4a_X m^5 T_R^3}{3\pi^5\Lambda_X^4}\,, \tag{S65}$$

and similar for scattering with $a_X \to 2d_X$ (note that for RH neutrinos there is only annihilation, provided that there are not in thermal equilibrium in the early universe). Summing the contributions from annihilation and scattering (including a factor of 2 for charge multiplicity), we obtain

$$R(m) = \frac{45\sqrt{5}M_{\rm Pl}}{\pi^{17/2} g_*^{3/2}(m)} \left(a_X + 4d_X\right) \frac{T_R^3}{\Lambda_X^4}\,, \tag{S66}$$

and finally

$$\Omega_\chi h^2 \approx 0.12\ \left(a_X + 4d_X\right) \left(\frac{m_\chi}{10\,\text{keV}}\right) \left(\frac{T_R}{4\,\text{MeV}}\right)^3 \left(\frac{1.6\,\text{TeV}}{\Lambda_X}\right)^4 \left(\frac{10.7}{g_*(m)}\right)^{3/2}\,, \tag{S67}$$

where we normalized to $g_*(T_R = 4\,\text{MeV}) = 10.7$, since this regime gives the dominant contribution to the abundance. Doing the integral of the collision term with the full cross-section, i.e. keeping finite $m_\chi = m_e \neq 0$, results in a scale that differs from the approximation above only by a few GeV. Directly solving the BE numerically with the full cross-section gives a difference of the same size, which demonstrates that the choice of $m = T_R$ is indeed appropriate. As discussed above we have neglected here the IR boundary term, which would change the result to $T_R^3 \to T^3 - T_{\rm IR}^3$. For $T_{\rm IR} \approx 1\,\text{MeV}$ and our default value $T_R = 4\,\text{MeV}$, this would merely amount to a 2% correction. Finally fixing $T_R = 4\,\text{MeV}$, the limit from DM overproduction reads for scalar and vector operators (valid for $m_\chi \ll T_R$)

$$\Lambda_S \gtrsim 1.7\,\text{TeV} \left(\frac{m_\chi}{10\,\text{keV}}\right)^{1/4}\,, \qquad \Lambda_V \gtrsim 2.3\,\text{TeV} \left(\frac{m_\chi}{10\,\text{keV}}\right)^{1/4} \tag{S68}$$

or

$$\frac{m_\chi^2}{4\pi\Lambda_S^4} \lesssim 4.1 \times 10^{-52}\text{cm}^2 \left(\frac{m_\chi}{10\,\text{keV}}\right)\,, \qquad \frac{m_\chi^2}{4\pi\Lambda_V^4} \lesssim 1.0 \times 10^{-52}\text{cm}^2 \left(\frac{m_\chi}{10\,\text{keV}}\right)\,, \tag{S69}$$

in good agreement with Fig. 1.

IV.c. UV Completions

For a light vector or scalar mediator X, in principle we would need to solve two coupled Boltzmann Equations for χ and X. However, since we are interested in the limit $T_R \ll m_V$ and unstable mediators, the mediator abundance is always negligible and we can treat X as a short-lived resonance and simply work with a single Boltzmann equation for χ (c.f. also Ref. [84]). Thus we can employ again the general result from Eq. (S62), using the collision term for the relevant process in the UV complete theory.

Since we expect significant deviations from the EFT calculation only in the resonant regime (i.e. when the mediator is produced on-shell) we restrict to annihilation. The corresponding s-channel cross-section for a vector mediator reads

$$\sigma_{e^+e^-\to\chi\overline{\nu}} = \frac{g_e^2 g_\chi^2 \sqrt{1-4m_e^2/s}}{48\pi\left((s-m_V^2)^2 + m_V^2\Gamma_V^2\right) s^2 (s-4m_e^2)} (s+2m_e^2)(s-m_\chi^2)^2(2s+m_\chi^2)\,, \tag{S70}$$

which results in the collision term (taking $m_\chi \ll m_e$)

$$\mathcal{C}_{e^+e^-\to\chi\overline{\nu}} = \frac{T}{8\pi^4} \int_{4m_e^2}^\infty \left(1-4m_e^2/s\right) s^{3/2} \sigma_{e^+e^-\to\chi\overline{\nu}} K_1\left(\sqrt{s}/T\right)\, ds\,, \tag{S71}$$

and the partial widths are given by

$$\begin{aligned}
\Gamma(V\to e\overline{e}) &= \frac{g_e^2 m_V}{12\pi}\left(1+2\frac{m_e^2}{m_V^2}\right)\sqrt{1-4\frac{m_e^2}{m_V^2}}\,,\\
\Gamma(V\to\chi\overline{\nu}) &= \frac{g_\chi^2 m_V}{12\pi}\left(1+\frac{m_\chi^2}{2m_V^2}\right)\left(1-\frac{m_\chi^2}{m_V^2}\right)^2\,.
\end{aligned} \tag{S72}$$

In the resonant limit that we are interested in, the dominant contributions come from $\sqrt{s} \approx m_V \gg m_e \gg m_\chi$. Therefore, we now set $m_\chi = m_e = 0$ and use the NWA for the cross-section, giving

$$\sigma_{e^+e^-\to\chi\overline{\nu}} \approx g_e^2 \pi \delta(s - m_V^2) \mathrm{BR}(V \to \chi\overline{\nu})\,, \tag{S73}$$

and thus

$$\mathcal{C}_{e^+e^-\to\chi\overline{\nu}} = \frac{g_e^2}{8\pi^3} m_V^3 T K_1\left(\frac{m_V}{T}\right) \mathrm{BR}(V \to \chi\overline{\nu})\,. \tag{S74}$$

Therefore the final integral becomes

$$\int_{m/T_R}^{\infty} x^4 \mathcal{C}_{e^+e^-\to\chi\overline{\nu}}(x) = \frac{g_e^2 m_V^3 m}{8\pi^3} \mathrm{BR}(V \to \chi\overline{\nu}) \int_{m/T_R}^{\infty} x^3 K_1\left(\frac{m_V}{m} x\right)\,. \tag{S75}$$

Now choosing $m = m_V$, and taking $m_V \gg T_R$, it is clear that the integral is again UV dominated, which justifies to integrate to $T = 0$ instead to some finite value. This gives for the asymptotic yield

$$R = \frac{135\sqrt{5} M_{\rm Pl}}{32 m_V \pi^{13/2} g_*^{3/2}(m_V)} \frac{g_e^2 g_\chi^2}{g_e^2 + g_\chi^2} \int_{m_V/T_R}^{\infty} x^3 K_1(x)\, dx\,, \tag{S76}$$

and finally for the relic abundance

$$\Omega_\chi h^2 = 0.12 \left(\frac{g_e g_\chi / \sqrt{g_e^2 + g_\chi^2}}{4.9 \times 10^{-12}}\right)^2 \left(\frac{m_\chi}{10\,\mathrm{keV}}\right) \left(\frac{10\,\mathrm{MeV}}{m_V}\right) \left(\frac{10.7}{g_*(m_V)}\right)^{3/2} K\,, \tag{S77}$$

with

$$K = \frac{2}{3\pi} \int_{m_V/T_R}^{\infty} x^3 K_1(x)\, dx\,, \tag{S78}$$

so that for $T_R \to \infty$, $K \to 1$, so that one recovers the usual IR freeze-in result from the decay of a particle V in the thermal bath [87]. Instead the finite reheating temperature result in additional suppression for increasing mediator masses, for example

$$\left(\frac{10\,\mathrm{MeV}}{m_V}\right) \left(\frac{10.7}{g_*(m_V)}\right)^{3/2} K = \begin{cases} 6.3 \times 10^{-1} & m_V = 10\,\mathrm{MeV} \\ 8.7 \times 10^{-5} & m_V = 50\,\mathrm{MeV} \\ 6.1 \times 10^{-10} & m_V = 100\,\mathrm{MeV} \end{cases}\,. \tag{S79}$$

Finally it is convenient to introduce $g_\chi \equiv \kappa g_e$, $\Lambda_V = m_V/(g_e\sqrt{\kappa})$ so that

$$\Omega_\chi h^2 = 0.12\, C_X A_X \left(\frac{2\kappa}{1+\kappa^2}\right) \left(\frac{1.4 \times 10^9\,\mathrm{GeV}}{\Lambda_X}\right)^2 \left(\frac{m_\chi}{10\,\mathrm{keV}}\right) \left(\frac{m_X}{10\,\mathrm{MeV}}\right) \left(\frac{10.7}{g_*(m_X)}\right)^{3/2} K\,, \tag{S80}$$

where we have generalized our result to include scalar mediators with C_X and A_X defined below Eq. (S43). Comparing to the limits in the EFT regime from the previous section, one can estimate the transition region by equating the abundances and solving for m_V, which gives for $m_\chi = 10\,\mathrm{keV}, T_R = 4\,\mathrm{MeV}$ the value $m_X \approx 160\,\mathrm{MeV}$, in good agreement with Fig. 3 and S2.